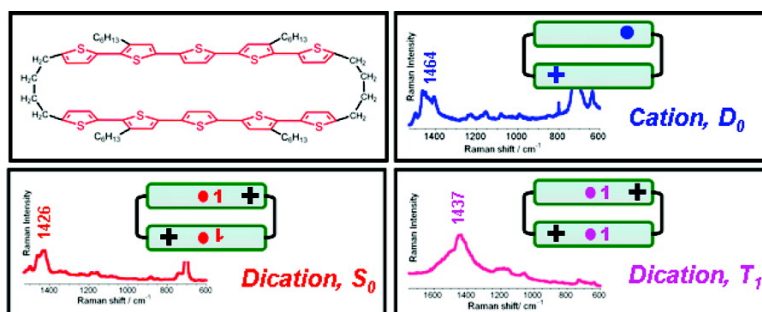## Communication

Raman Spectroscopy Shows Interchain through Space Charge Delocalization in a Mixed Valence Oligothiophene Cation and in Its #-Dimeric Biradicaloid Dication

Juan Casado, Kazuo Takimiya, Tetsuo Otsubo, Francisco J. Ramírez, J. Joaquín Quirante,
Rocío Ponce Ortiz, Sandra R. Gonza#lez, María Moreno Oliva, and Juan T. Lo#pez Navarrete

More About This Article

Additional resources and features associated with this article are available within the HTML version:

- Supporting Information
- Access to high resolution figures
- Links to articles and content related to this article
- Copyright permission to reproduce figures and/or text from this article

View the Full Text HTML

Raman Spectroscopy Shows Interchain through Space Charge Delocalization in a Mixed Valence Oligothiophene Cation and in Its π-Dimeric Biradicaloid Dication

Juan Casado,*,[†] Kazuo Takimiya,[‡] Tetsuo Otsubo,[‡] Francisco J. Ramírez,[†] J. Joaquín Quirante,[†] Rocío Ponce Ortiz,[†] Sandra R. González,[†] María Moreno Oliva,[†] and Juan T. López Navarrete*,[†]

Departamento de Química Física, Universidad de Málaga, 29071-Málaga, Spain, and Department of Applied Chemistry, Graduate School of Engineering, Hiroshima University, Higashi-Hiroshima 739-8527, Japan

Received August 7, 2008; E-mail: casado@uma.es; teodomiro@uma.es

Any new electronic insight on charge transfer processes, though subtle at first glance, can contain key information for optimal development of new organic materials. Hence how charge delocalizes over a given molecule or substrate acquires utmost importance. Mixed-valence (MV) systems are interesting models for charge transfer events where two equal redox centers in different oxidation degrees compete for the charge via a mediating molecular bridge.[1] In particular, class III MV (Robin–Day classification) compounds are very promising in application as single-molecule devices or molecular wires[2] where the excess of charge is fully delocalized in the two redox centers over the conjugated bridge, or *through-bond* electronic communication.[3] The counterpart class II MV systems are characterized by the localization of the total charge in one of the donor groups. Much less attention however has been devoted to class III MV cases where *through-space* intercenter full charge delocalization takes place. A paradigmatic case of the latter is π-dimerization of conjugated radical cations.[4] Recently, these π-dimers have been suggested to possess very accessible magnetically active triplet states,[5] a phenomenon similar to the polaron pair versus bipolaron stability debate, occurring in extensive *through-bond* electron delocalized molecules (long chain oxidized oligothiophenes), owing to their biradicaloid nature.[6] Interest in electron delocalization aside, the realization of intermolecular charge delocalization, and magnetism is highly welcome for new functional materials.

Nonetheless, in π-stacked molecules the degree of cofacial intermolecular coupling determines the extent of the interaction and the appearance of the properties mentioned above. A decathiophene[7] constituted by two parallel π-stacked pentathiophenes (5T) spaced by four methylenes spacers, [4,4] in Figure 1, is our target molecule and provides an opportunity to address the features of *through-space* electronic coupling in (i) class III MV systems when it is charged to the radical cation and (ii) its π-dimeric dication to explore the biradicaloid character and the presence of triplet magnetic states. We want to check the spectroscopic signals of *through-space* charge delocalization such as the existence of the Davidov effect or the occurrence of singlet biradicaloid species. In all these cases, Raman spectroscopy pivots a common argument with the challenge of providing the characteristic spectra of every species. As an experimental guide DFT model chemistry is used to analyze the vibrational data.

The spectra of a single chain pentathiophene (i.e., **5T** or α,ω-dimethyl pentathiophene in Figure S1) in the radical cation (**5T**[•+]) and dication (**5T**[+2]) states are considered as references showing the strongest Raman lines at 1438 and 1417 cm^{−1}, respectively (Figure
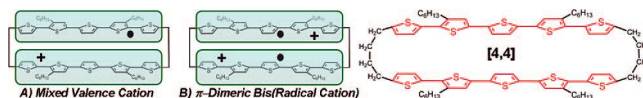

Figure 1. Chemical structure and notation. Models A and B schematize the cases where inter-**5T** interactions take place.
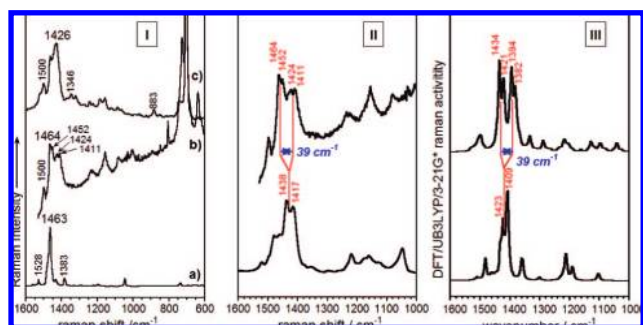

Figure 2. (i) (a and c) 1064 nm FT-Raman spectra of [4,4] and [4,4][+2] and (b) 785 nm resonant Raman spectrum of [4,4][•+]. (ii) Experimental Raman spectra of the radical cations of **5T** (bottom) and [4,4] (top). (iii) DFT/UB3LYP/3-21G* theoretical Raman spectra of **5T**[•+] (bottom) and [4,4][•+] (top).

S2).[8] Considering that the spectrum of neutral **5T** has the strongest signal at 1481 cm^{−1}, the underlying structural motif causing this spectral evolution with oxidation is the quinoidization of the π-conjugated backbone which is more pronounced for higher charged species. In oxidized [4,4] the spectra (Figure 2) were acquired by using resonance Raman spectroscopy with 785 and 1064 nm excitation wavelengths, matching the absorptions of [4,4][•+] at 760 nm and that of [4,4][+2] at 1085 nm, respectively (Figure S3).

The 785 nm spectrum of [4,4][•+] shows the stronger peaks at 1464−1452 cm^{−1} at higher values than that in **5T**[•+] at 1438 cm^{−1}. After two-electron extraction in [4,4][+2] the band that becomes stronger in the 1064 nm spectrum is at 1426 cm^{−1} between **5T**[•+] and **5T**[+2]. From a structural point of view, one can argue that pentathiophene quinoidizations in [4,4][•+]/[4,4][+2] are substantially lower than the ones attained in single **5T**[•+]/**5T**[+2] chains.

As for the radical cations, this finding can be interpreted as a result of charge delocalization in the two chains promoted by the competition between the two donors leading to *through-space* mixed valence action. The radical cation can be viewed as a molecular domain of 10 like interacting thiophenes (i.e., 5T+5T) where one charge is fully delocalized relaxing the quinoidal modification relative to **5T**[•+] with the subsequent Raman upshift. For [4,4][+2], again each charge does not totally reside on one 5T chain but apparently delocalizes in the two since quinoidization is greater than that in **5T**[•+] and lower than that in **5T**[+2]. In this case the driving force for the interaction is the
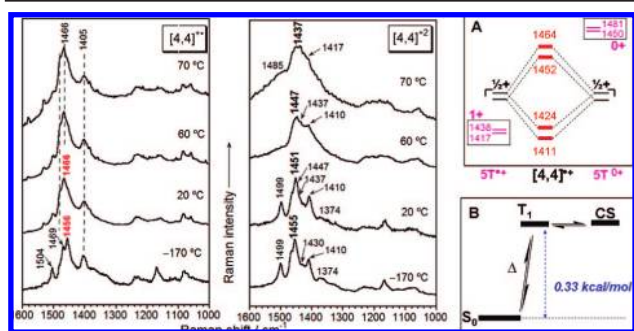
Figure 3. Solid state Raman spectra as a function of temperature for **[4,4]**$^{\bullet+}$ (785 nm excitation) and **[4,4]**$^{+2}$ (633 nm excitation). (A) Vibrational coupling in the class III MV **[4,4]**$^{\bullet+}$. (B) Thermal equilibrium in **[4,4]**$^{+2}$.

energetic gain coming from the formation of a *new* interchain bond by π-dimerization. The situation is equivalent to the full *through-space* delocalization of two charges in 10 rings (i.e., 5T+5T) such as in the cations. Theoretical charges and optimized geometries (Figure S4) support the spectroscopic interpretation. In addition, it must be highlighted that the average distance between the two 5T chains is reduced from 4.86 Å in neutral **[4,4]** to 4.26 Å in **[4,4]**$^{\bullet+}$ in line with the interchain coupling (see Figure S4c for additional details). As for **[4,4]**$^{+2}$, we have analyzed the charge electronic density according to the AIM theory by Bader,[9] fully characterized the bond critical points in the inter-5T region, and found interchain C···C interactions (Figure S4) predicted to be particularly strong in the dication species.

Looking in more detail at the spectra, we observe that the strong modes of the 785 nm spectrum of **[4,4]**$^{\bullet+}$ correspond to a double doublet at 1464, 1452, 1430, 1408 cm^{-1} which is very well reproduced by theory with peaks at 1434, 1421, 1394, 1382 cm^{-1} in Figure 2. This spectral property must be interpreted as the result of the motional coupling of the two 5T chains giving rise to four vibrational bands coming from the two doublets on **5T**$^{\bullet+}$ (i.e., 1438 and 1417 cm^{-1}). The 39 cm^{-1} splitting reveals a regime of strong vibronic coupling between the two parallel chains, an electron-vibrational interaction that takes place between the chains bearing approximately a half-positive charge (see Figure S4) that nicely provides the vibrational states distribution proposed in Figure 3A (Figure S5 for the normal modes). This is a phenomenon similar to the crystal splitting of electronic bands by the Davidov effect owing to molecular stacking in the crystalline cell, the amount of it being related with the extent of the interaction.[10] The evolution of this phenomenon in **[4,4]**$^{\bullet+}$ has been followed thermally in Figure 3 as the strongest peak moves down from 1466 cm^{-1} at 20 °C to 1456 cm^{-1} at −170 °C. This is uncommon and might be ascribed to a new MV property, in particular to the class III→class II transition by cooling. Short chain radical cations belong to class III fully delocalized MV systems, while long chain derivatives show electron localization (class II).[11] Thermal transition between the two classes is observed in borderline class III/class II molecules (Figure S6) such as in our **[4,4]**$^{\bullet+}$. This transition might provoke a localization of the charge in one of the two chains leading to a larger 5T quinoidization likely at the origin of the Raman downshift.

For the dications, the two interacting SOMO orbitals (Figure S7) are clearly disjoint (each SOMO is in one chain without overlapping), an orbital property established for biradicaloid species meaning that interchain coupling might induce biradical character to the S$_0$ which might result in a singlet biradical species.[12] We have calculated the energy difference between the close- and open-shell singlet structures for **[4,4]**$^{+2}$ finding the biradical open-shell form more stable by 4.89 kcal/mol. If we focus on a singlet

biradical, then the presence of a triplet biradical state (i.e., T$_1$) near the S$_0$ is mandatory. We have optimized the T$_1$ geometry for **[4,4]**$^{+2}$ located 0.33 kcal/mol over the S$_0$ which prompts us to explore it by Raman thermospectroscopy. According to the energetic diagram in Figure 3, heating the sample would populate the T$_1$ supposing a decrease of the electronic communication (spin decoupling by low exchange energy), closely followed by a full charge separation or interchain disconnection (CS or charge separated state in Figure S8 where the two positive charges are "isolated" in one chain each). This is consistent with the spectral downshift of **[4,4]**$^{+2}$ by heating (Figure 3) leading to a strong and broad line peaking at 1437 cm^{-1} (similar to the 1438 cm^{-1} line in **5T**$^{\bullet+}$). This interpretation agrees with the following findings: (i) From the theoretical spectrum of S$_0$ (peak at 1425 cm^{-1}) to that of T$_1$ (peak at 1406 cm^{-1}) a downshift of 19 cm^{-1} is predicted in agreement with the 18 cm^{-1} experimental one (i.e., 1455→1437 cm^{-1}) (Figure S9); (ii) The Raman response of **[4,4]**$^{\bullet+}$ is invariant in the high temperature range; (iii) The most notable spectral changes on **[4,4]**$^{+2}$ occur at high temperatures in a relatively small interval (i.e., 20−70 °C) likely enough to modify the spectra by the S$_0$↔T$_1$↔CS equilibrium considering the small 0.33 kcal/mol singlet-to-triplet energy difference; (iv) The thermal cycle is fully reversible; (v) Cooling causes a better resolution of the **[4,4]**$^{+2}$ singlet biradical spectrum in agreement with it being the S$_0$. (vi) The small S$_0$↔T$_1$↔CS energy difference can lead to spectral broadening of a feature observed in the 70 °C spectrum. This does not occur in **[4,4]**$^{\bullet+}$ with a D$_0$↔CS energy difference of 10.60 kcal/mol (Figure S7).

In summary, we have found Raman fingerprints of the following: (i) *through-space* charge delocalization in the radical cation of a decathiophene owing to mixed valence action with Raman Davidov-like splitting (stacking property) and class III→class II transition on cooling; (ii) *through-space* charge delocalization in the dication providing biradicaloid character to its S$_0$ yielding thermally accessible triplet states. This demonstrates the great power of Raman spectroscopy for the understanding of fundamental insights of electronic processes in organic conjugated materials exploitable in molecular electronics.

Supporting Information Available: More data and explanations together with the calculated geometries and total energies. This material is available free of charge via the Internet at http://pubs.acs.org.

References

(1) Robin, M. B.; Day, O. *Adv. Inorg. Chem. Radiochem.* **1967**, *10*, 247.
(2) Tour, J. M.; Kozaki, M.; Seminario, J. M. *J. Am. Chem. Soc.* **1998**, *120*, 8486. Davies, W. B.; Svec, W. A.; Ratner, M. A.; Wasielewski, M. R. *Nature* **1998**, *396*, 60.
(3) For example, see: Coropceanu, V.; Cornil, J.; Da Silva Filho, D. A.; Olivier, Y.; Silbey, R.; Bredas, J.-L. *Chem. Rev.* **2007**, *107*, 2165.
(4) Miller, L. L.; Mann, K. R. *Acc. Chem. Res.* **1996**, *29*, 417.
(5) Yamazaki, D.; Nishinaga, T.; Tanino, T.; Komatsu, K. *J. Am. Chem. Soc.* **2006**, *128*, 14470.
(6) For example: van Haare, J. A. E. H.; Havinga, E. E.; van Dogen, J. L. J.; Janssen, R. A. J.; Cornil, J.; Brédas, J. L. *Chem.−Eur. J.* **1998**, *4*, 1509.
(7) Sakai, T.; Satou, T.; Kaikawa, T.; Takimiya, K.; Otsubo, T.; Aso, Y. *J. Am. Chem. Soc.* **2005**, *127*, 8082.
(8) Casado, J.; Hernández, V.; Hotta, S.; López Navarrete, J. T. *Adv. Mater.* **1998**, *10*, 1258; *J. Chem. Phys.* **1998**, *109*, 10419.
(9) Bader, R. F. W. *Atoms in Molecules. A Quantum Theory*; Clarendon Press: Oxford, 1990.
(10) Muccini, M.; Lunedei, E.; Taliani, C.; Beljonne, D.; Cornil, J.; Brédas, J. L. *J. Chem. Phys.* **1998**, *109*, 10513. Cornil, J.; Beljonne, D.; Brédas, J. L. *Adv. Mater.* **2001**, *13*, 1053.
(11) Lacroix, J. C.; Chane-Ching, K. I.; Maquère, F.; Maurel, F. *J. Am. Chem. Soc.* **2006**, *128*, 7264.
(12) Borden, W. T.; Iwamura, H.; Berson, J. *Acc. Chem. Res.* **1994**, *27*, 109.

JA806207J